WATER RESOURCES RESEARCH, VOL. 36, NO. 1, PAGES 355–360, JANUARY 2000

Glass casts of rock fracture surfaces: A new tool for studying flow and transport

Jiamin Wan, Tetsu K. Tokunaga, Thomas R. Orr, Jim O'Neill, and Robert W. Connors

Earth Science Division, Lawrence Berkeley National Laboratory, Berkeley, California

Abstract. A method was developed for fabricating transparent glass casts of fractured rock pairs. These glass casts provide reproduction of surface topography and roughness of natural fractures, optical clarity, and representative wettabilities of mineral surfaces. The glass casts are an improved tool for studying flow and transport in fractures compared to previous approaches. The surface of a clean glass fracture has a contact angle near zero, and more importantly, the surface wettability can be intentionally altered with chemical treatment. Glass casts of rock fracture surfaces may be used for visually and quantitatively studying various physical, chemical, and microbial processes occurring in rock fractures, especially when multiple fluid phases are involved.

1. Introduction

Laboratory studies of flow and transport in fractured rock systems can provide mechanistic insights into larger-scale phenomena which are critical in many areas, such as flow and transport around repositories for high-level nuclear wastes, contaminant migration and remediation, and enhanced petroleum recovery. Laboratory flow experiments employing transparent fracture replicas permit direct visual investigation of flow processes within the fracture plane and identification of controlling mechanisms. Fracture flow visualization experiments have been conducted in parallel rough surface glass plates [e.g., *Fourar et al.*, 1993; *Nicholl et al.*, 1994; *Nicholl and Glass*, 1994], glass micromodels [e.g., *Haghighi et al.*, 1994; *Wan et al.*, 1996], and epoxy casts of natural fractures [*Gentier*, 1986; *Gentier et al.*, 1989; *Hakami and Barton*, 1990; *Persoff and Pruess*, 1995; *Cox et al.*, 1995; *Geller and Pruess*, 1995; *Brown et al.*, 1998]. Rough glass plates and glass micromodels provide a means of isolating flow processes from aperture heterogeneity and water-wetting characteristics similar to many rock surfaces but do not represent actual natural fractures. Fracture casts made with epoxy resin can provide reasonably accurate reproduction of natural fracture aperture fields but have hydrophobic surfaces. This latter characteristic constrains the usefulness of epoxy casts in studies of partially saturated water statics and flow to investigations involving hydrophobic interactions. The epoxy casts also have some other limitations such as lower stiffness, local deformation, long-term creep, absorption of dyes, and temporal changes in surface chemistry. In this paper, a new method is presented for replicating natural rock surface topography using molten glass. Glass casts have the combined advantages of closely reproducing natural fracture surface roughness, being treatable to provide the wide range of wettabilities found for natural rock surfaces, and lessening some of the problems associated with epoxy replicas. Comparisons between measured surface profiles of original rock fractures and glass casts are provided, along with measurements of surface transmissivities and wettabilities.

Paper number 1999WR900289.

2. Glass Casting Technique

Suitable original rock fracture samples from which casts are to be made are selected with an awareness of limitations inherent to casting methods. Original fracture surfaces need to be competent (nonfriable) and free of vugs. A pair of matched rock slabs separated by such a fracture can permit casting of glass replicas. The materials used for making glass fracture casts are silicone rubber and catalyst 8 (Dow Corning Incorporated, Midland, Michigan), Pam "no stick" cooking spray (Boyle-Midway Household Products, Incorporated, New York, New York), casting wax (Rio Jade KC, Rio Grande Company, Albuquerque, New Mexico), investment powder (Kerr Satin Cast 20, Kerr Manufacturing Company, Romulus, Michigan), and glass (Corning Glass 010, Corning Incorporated, Corning, New York).

The casting procedure involves five steps; the first is to make silicone rubber molds (negatives) of each rock slab. Silicone rubber and catalyst 8 are mixed at a mass ratio of 10:1, and the mixture is evacuated for 5 min at a gauge pressure of -95 kPa to remove air bubbles. The working time of the mixture is 50 min, and the curing time is 24 hours. The rock fracture surfaces are sprayed with a thin layer of Pam to facilitate separating. Each half of the rock fracture is placed in a container, submerged under the rubber mixture, and re-evacuated for 2 min. After 24 hours of curing at room temperature, the molds are separated from the rocks. These silicone molds are reusable.

In step 2, wax positives are made from the silicone rubber molds. The casting wax is melted on a hot plate at 65°C. The liquid wax is poured into the prewarmed (50°C) silicone molds and allowed to cool to ~30°C. The two halves of wax replicas of the rock fracture are then released from the silicone molds. The wax positives can easily change their shape during cooling and result in warping. To minimize warping during casting, the two halves of wax replicas are matched together immediately and put under a flat weight until cooled to room temperature.

In step 3, investment molds (negatives) are made from the wax positives. The investment powder used in this study is composed of crystalline silica and gypsum, with particle sizes <10 μm and 90% finer than 1 μm. Water is added to the

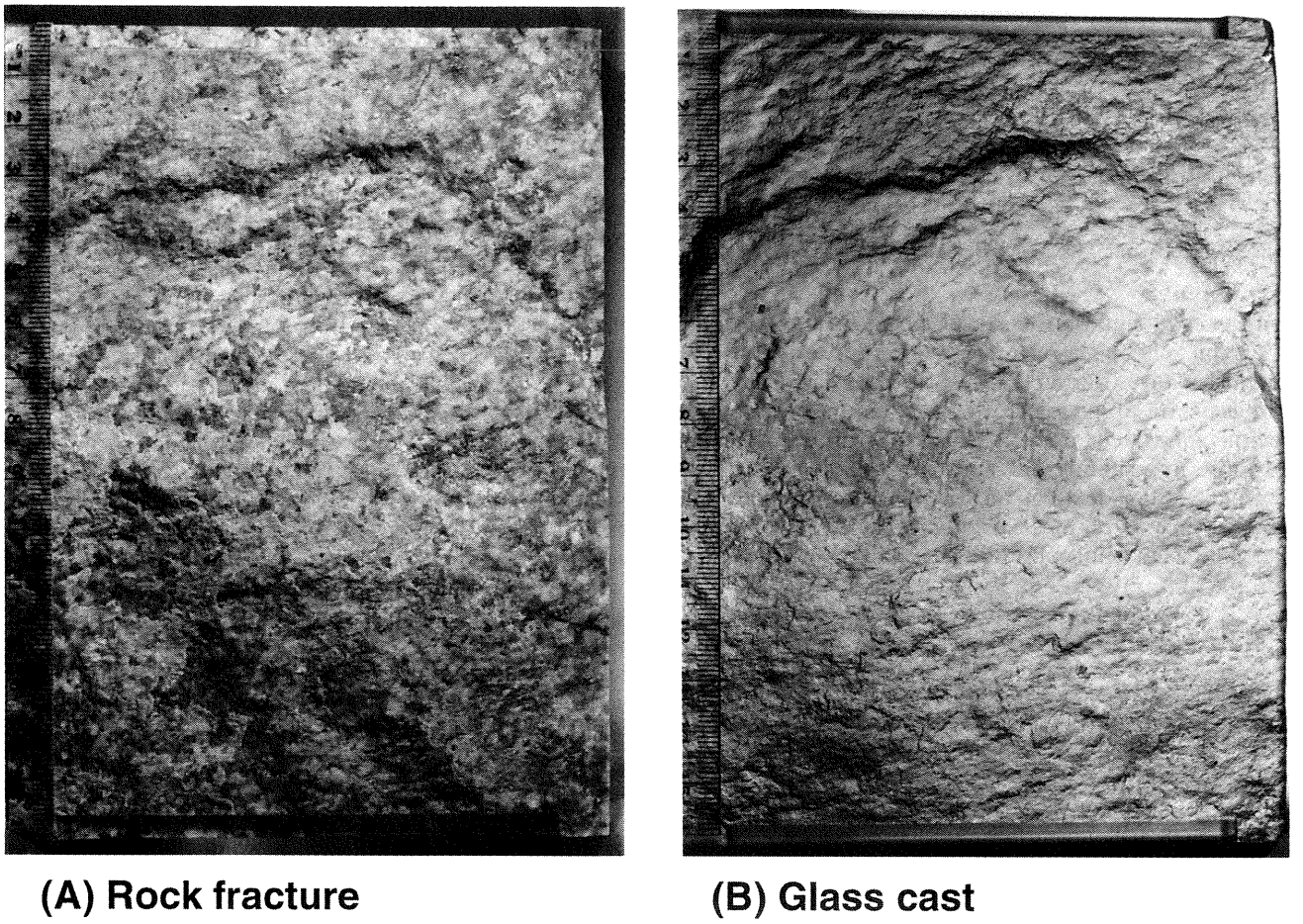

Figure 1. Photographs of the surface of (a) a granite fracture and (b) its glass cast. These examples are both 120 mm by 160 mm.

investment powder in a ratio of 38 mL per 100 g of powder, and the mixture is evacuated (−95 kPa) for 2 min. Each wax pattern is placed face up in a container consisting of a steel frame set on top of a supporting steel plate. The investment mixture is poured into the container, evacuated (−95 kPa) for 2 min, and then returned to atmospheric pressure and room temperature for 24 hours. Kerr Satin Cast 20 has an approximate working time of 9 min and a cure time of ~24 hours. After removing the supporting steel plate, the steel frame (with wax positives and investment) is inverted and loaded into a furnace with the wax side up. The wax burn-off process is accomplished in a series of temperature steps (149, 315, 482, and 732°C), with each step lasting for 2–4 hours. After burning off the wax pattern, the investment molds are obtained. The framed molds are kept in the furnace at 500°C until melted glass is ready to be poured in.

In step 4, glass fracture casts (positives) are made from the investment molds. Glass is crushed into centimeter-sized pieces and melted in a ceramic crucible at a temperature of 983°C for 24 hours. The framed molds are placed on top of a ceramic vacuum plate in preparation for glass casting. Glass is poured into the framed investment molds and then a vacuum (−95 kPa) is applied to the ceramic plate for ~60 s as the glass flows and fills the molds. The framed glass mold sets are then annealed at 432°C for 4 hours. The furnace is then slowly cooled to room temperature, after which the glass casts are released from the investment molds in warm water (the investment molds are not reusable).

The final step entails finishing the glass fracture replicas. In order to improve optical clarity the surface opposite the fracture is ground flat. Any excessive thickness of the glass casts resulting from step 4 is removed. A minimum thickness of 3–5 mm (at the thinnest points) is preferred for each half, but the final overall thickness will depend on the fracture topography. Five sides (four edges and the back) of each half cast are ground and polished as a pair. If highly water wettable surfaces are desirable, the glass casts are subjected to two more treatments. First, the casts are soaked overnight in concentrated nitric acid, water rinsed, and dried. Then, the casts are placed into a furnace, heated up at a rate of 10°C min^{-1}, and brought up to 420°C for 1 hour to bake off any residual hydrophobic coating. The casts are allowed to cool to room temperature overnight in the furnace. This treatment results in surfaces with nearly zero contact angles for water.

In our discussion, we refer to three sets of casts. The first replicated a Swedish granite (120 mm by 160 mm). A photograph of one side of the granite fracture (Figure 1a) and its corresponding finished glass fracture cast (Figure 1b) qualitatively shows reproduction of fracture surface texture and roughness. Reflected light was used for photographing the rock, while only transmitted light photography was suitable for the glass cast (because of strong reflections and glare under

reflected light). Because of differences in lighting, these photographs do not provide a good visual comparison of the detailed surface textures. A second (70 mm by 70 mm) cast replicated a fractured gabbro (Dixie Valley, Nevada) that has been previously cast in epoxy [*Power and Tullis*, 1989; *Persoff and Pruess*, 1993]. In addition to these casts of natural fractured rock, glass casts were also made of quartz glass surfaces (1 cm^2 in bulk surface area) roughened with corundum for the purpose of determining limitations of casting with respect to fine-scale roughness.

3. Characterization of Glass Fracture Casts

The topography of a glass cast surface was compared with that of the original rock fracture over selected areas using laser profilometers and an atomic force microscope (AFM). For coarse-scale measurements, surfaces were profiled with an LK-081 CCD laser displacement sensor (Keyence Corporation, Woodcliff Lake, New Jersey) mounted on a View Precis 3000 coordinate measuring machine (View Engineering Division, General Scanning Incorporated, Simi Valley, California). The LK-081 laser has a vertical (z) measurement range of 30 mm, a spot diameter of ~70 μm, and an uncertainty of $\pm$35 μm in z. For higher-resolution measurements over smaller areas and narrower topographic ranges on rock and glass casts, a UBM laser (UBM, Sunnyvale, California) was used instead of the LK-081. The UBM laser has a spot size of 1 μm, a z measurement range of 100 μm, and a z resolution of 0.06 μm. This system was also used to obtain surface profiles on the roughened quartz glass samples. The View Precis 3000 used on both of these laser systems has resolution and repeatability in the x-y plane better than (less than) 3 μm. For higher-resolution topography, small areas of glass casts and roughened glass surfaces were scanned with an AFM (Autoprobe M5, Park Scientific Instruments, Sunnyvale, California). We used this AFM in the standard contact scanning mode to obtain information on finer-scale topography and also to obtain values of surface roughness for comparison with laser profilometry results. The Autoprobe M5 has a resolution of 0.025 nm and lateral range of 100 μm by 100 μm. However, since the maximum measurable z variation of this AFM is only 8 μm, scans on rough surfaces must be confined to even smaller areas than the instrument's 100 μm by 100 μm range.

Wettability was qualitatively evaluated by placing water droplets on surfaces and observing whether or not spontaneous spreading occurred. Further comparisons of wettabilities were obtained through water imbibition experiments into the Dixie Valley fracture pairs (gabbro, glass, and epoxy). Each fracture pair was confined in retaining frames with a common average stress of ~23 kPa applied with a set of eight compression springs, in a manner similar to that used by *Persoff and Pruess* [1995]. A more controlled method of applying the normal stress on transparent fractures has been described by *Nicholl et al.* [1994] but was not used here. The brass retaining frames prevented direct viewing of the fracture boundaries but permitted observation of most of the transparent fracture casts during experiments. Since we did not employ radiometric or tomographic methods, the extent of wetting in the opaque rock fracture could only be inferred after opening up the system at the end of an experiment. Each fracture plane was oriented vertically, and the lower edge was placed in contact with a free water surface; remaining boundaries were left open to atmosphere pressure. Water freely imbibed into the gabbro and glass fractures upon contact with the water surface. Since spontaneous imbibition did not occur in the epoxy cast, its bottom edge was progressively lowered into the water reservoir until a slight amount of wetting was observable. For purposes of photographic comparisons of imbibition, a blue dye tracer (Liquitint Patent Blue, Chromatech Incorporated, Plymouth, Michigan) was added to the water. The extent of fracture wetting was compared after 60 min of imbibition. The rock fracture was opened up and photographed to obtain a record of the wetting phase distribution. While wetting was directly observable in the mated glass and epoxy casts, these too were opened up and photographed at the end of the imbibition test for more direct comparison with the rock fracture.

Finally, a set of comparisons between average apertures and permeabilities of the original granite rock fracture and three pairs of glass casts were obtained. For these determinations, fracture pairs were confined in retaining frames with an approximately common normal stress of 5.7 kPa applied with a set of 12 compression springs located along the perimeter of the frame. Average apertures were determined by dividing the mass of water in saturated fractures by the density of water and the macroscopic fracture area. Permeabilities were obtained by the falling head method, with sealed lateral boundaries.

4. Results and Discussion

The glass cast pairs produced by our method matched without detectable shifting or rocking when placed together and had tight matching when paired with opposing rock surfaces. Being effectively solid at room temperature, the glass casts are not as easily deformable as epoxy casts when subjected to compression stress. However, because of some loss of very fine scale detail and some uncontrolled strain during the fabrication process, fracture surface topographies are not exactly reproduced.

Differences between casts and original rock surfaces were quantified through surface profile measurements. In Figure 2a, typical coarse-scale (100 mm line scans in 50 μm in-line steps at 60 mm lateral line separation) laser profiles of a rock surface and glass cast are compared. The root-mean-squared roughness (rmsr) values of the cast along these two profiles (2.22 and 1.14 mm) are very similar to that of the rock original (2.25 and 1.04 mm). However, since the rmsr is strongly influenced by larger-amplitude features encountered at larger distances, comparisons over shorter intervals are needed to obtain more direct information on replication of finer-scale features. Example profiles of the fracture and cast surface over shorter distances (10 mm lengths) are shown in Figure 2b. Note that the rmsr values are substantially lower than in the longer profile scans and that rock and glass casts still yield similar rmsr values, ranging from 0.63 to 0.84 mm. The scale dependence of the rmsr of natural fractures is well established, with larger-scale measurements having larger rmsr [*Power and Tullis*, 1991; *Brown*, 1995]. Results such as those shown in Figures 2a and 2b indicated that higher-resolution profiles were needed in order to quantify the roughness scale at which glass casting fails to replicate original fracture topography. However, precise colocation of points on rock and corresponding glass cast surfaces necessary for meaningful high-resolution scanning comparisons was not practical.

Since it was not practical to colocate points accurately enough on the original fractures and glass casts for purposes of comparing very fine scale roughness, these comparisons were

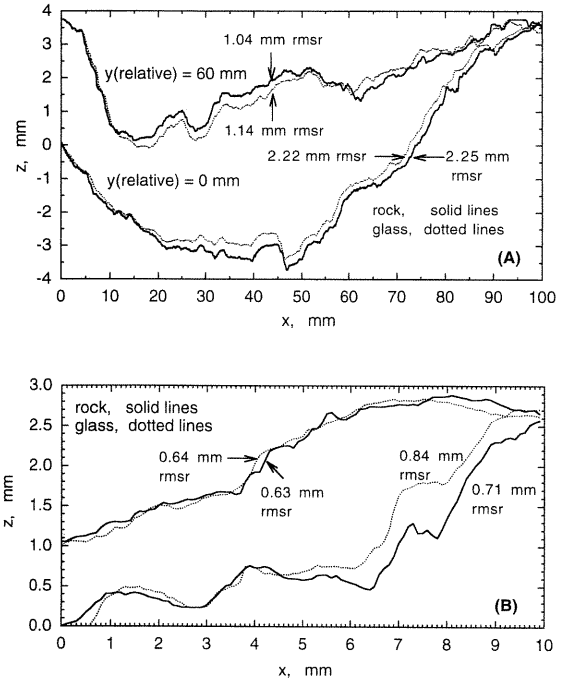

Figure 2. Comparisons of laser surface profiles on the granite fracture and glass cast. These (a) 100 mm and (b) 10 mm long profiles were measured in 50 μm steps.

made on the artificially roughened glass surfaces and their respective casts. The artificially roughened glass surfaces are macroscopically flat, such that they do not exhibit scale-dependent roughness over distances greater than ~1 mm. Thus profiles taken at randomly selected locations on a given sample are expected to be statistically identical, and precise colocation of corresponding points on originals and their casts is not required. The smoother quartz glass reference surface and its corresponding glass cast had laser-measured rmsr values of 0.16 and 1.52 μm, respectively, for profiles longer than 1000 μm (Figure 3, lower profiles). For purposes of checking laser measurements against the contact AFM, which only scan up to 100 μm profiles, rmsr values obtained over this shorter distance were also calculated for the laser data. The average rmsr obtained from 100 μm profiles were 0.13 and 1.51 μm for the smoother quartz glass surface and glass cast, respectively. The AFM yielded corresponding rmsr values of 0.10 and 1.0 μm, respectively, showing fair agreement with the laser measurements. The comparison of the smoother quartz glass surface and its glass cast reveals a potential problem which would arise in trying to replicate very smooth surfaces. A residual roughness is introduced in the casting method, probably due to the particle size of the investment powder. The laser measurements on the rougher quartz glass surface and its glass cast yielded rmsr values of 4.1 and 6.5 μm, respectively (Figure 3, upper profiles). These surfaces were too rough for AFM scanning at lengths greater than ~20 μm, so comparisons between laser and AFM measurements were not obtained. The results from the glass casts of these reference surfaces show that the method of glass casting produces surfaces with artificial roughness features in the nominally 1–5 μm range. This artificial roughness may only be problematic when attempting to replicate very smooth original surfaces.

The average aperture and transmissivity of the granite fracture pair under 5.7 kPa average stress were 122 μm and 6.1 $\times$ 10^{-7} m^2 s^{-1}, respectively. Three glass casts of this granite fracture pair were molded. The average apertures of three different glass cast pairs were 75, 173, and 255 μm under the same average normal stress. Transmissivities of these three glass cast pairs were 2.1 $\times$ 10^{-7}, 1.0 $\times$ 10^{-6}, and 1.9 $\times$ 10^{-6} m^2 s^{-1}, respectively. All average apertures and transmissivities were determined with a relative uncertainty of $\pm$5%. The 75 and 173 μm aperture fracture casts are good representations of the original system, but the 255 μm aperture fracture cast seems slightly warped. The artifact of slight bowing of one surface relative to its opposing surface tends to increase the cast transmissivity. *Reimus et al.* [1993] observed a change in hydraulic aperture in a natural fracture by a factor of 2 when it was disassembled and reassembled between trials. For purposes of observing flow and transport under a given cast aperture field this is not problematic.

When transparent fracture replicas are used in studies of multiphase fluid statics and flow, accurate reproduction of surface wettability is a very important factor. Epoxy cast surfaces are quite hydrophobic. Water "wets" dry epoxy surfaces with contact angles of ~90° (Figure 4a). In contrast, clean glass cast surfaces provide excellent water wettability, with near-zero contact angle (Figure 4b). When a surface with a contact angle greater than zero is required, the fracture surface can be treated with organosilanes [*Bethel and Calhoun*, 1953; *Jennings*, 1957; *Gatenby and Marsden*, 1957]. The covalent bond between the organosilane and the glass surface is reported to be quite stable. The different organic functional groups of different silanes and the concentration of the silane used for reaction can be varied to obtain different degrees of wettability.

As previously mentioned, water freely imbibed into both the gabbro fracture and its glass cast. Opening up the rock fracture revealed that ~70% of its surface was wetted (~50 mm) by the end of the 60 min test (Figure 5a). The glass cast showed a similar extent of average wetting but with a somewhat different wetting phase distribution (Figure 5b). The smoother wetting front observed on the rock relative to the glass cast may reflect the combined influences of finer-scale roughness, higher wettability, and perhaps matrix imbibition. The glass cast shown in Figure 5 was not subjected to the bake-off treatment for enhancing wettability; hence it contained several localized trapped dry surface zones. Glass casts subjected to such bake-off treatment are completely wettable. Imbibition into the ep-

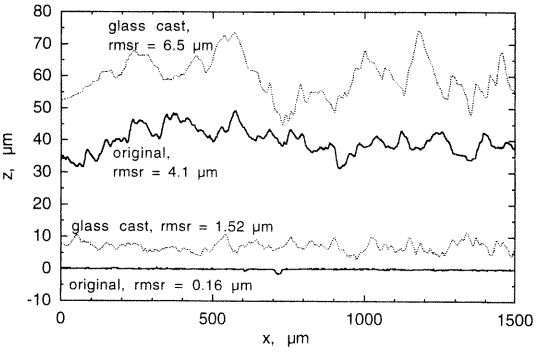

Figure 3. Comparisons of laser-measured surface profiles on artificially roughened quartz glass and glass cast surfaces at finer resolution.

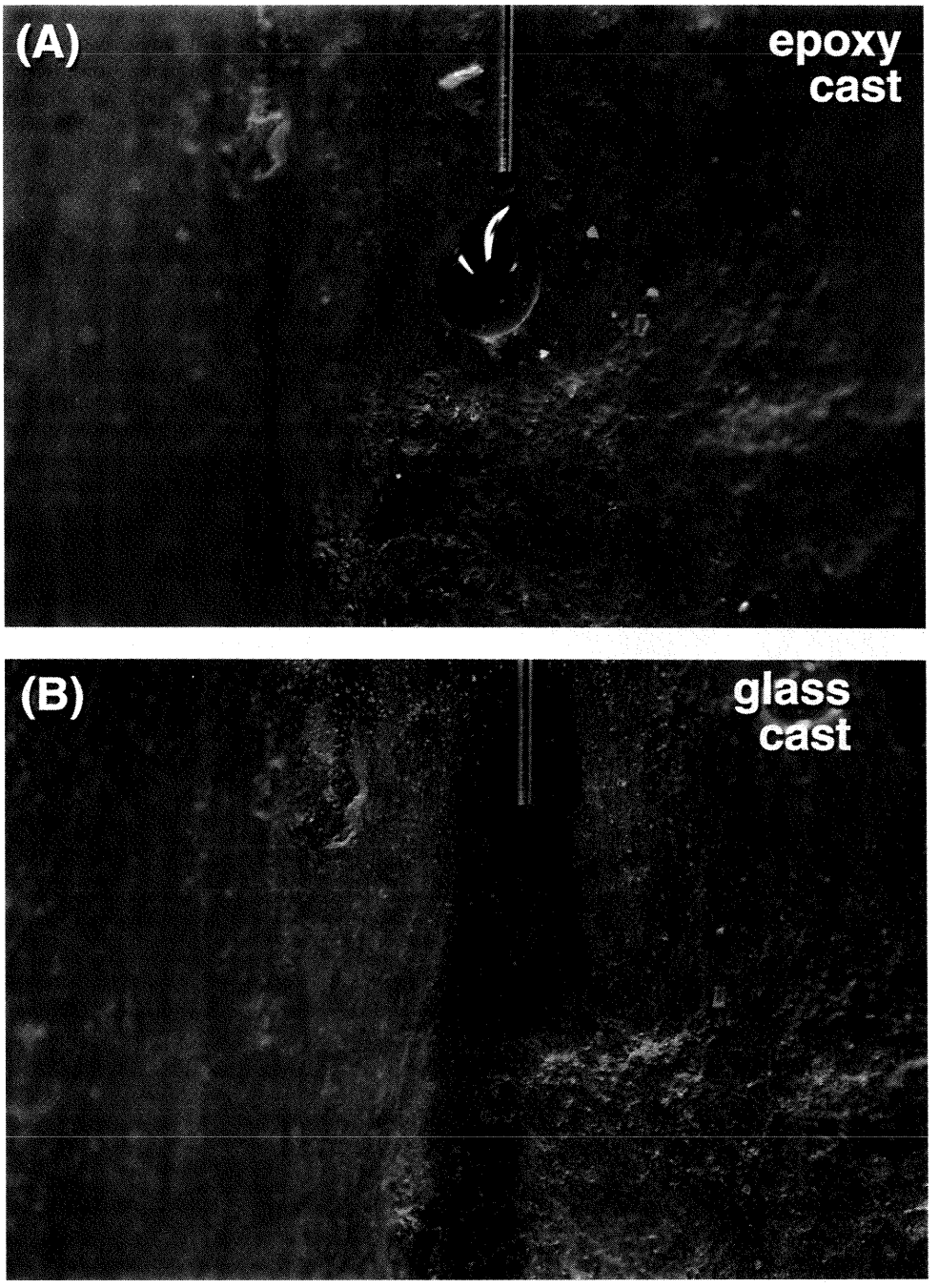

Figure 4. A comparison of surface wettability between an epoxy and a glass fracture cast. (a) A drop of water on fracture surface of an epoxy cast, where the contact angle is ~90°. (b) A drop of water on fracture surface of a glass cast, where the contact angle is near zero degrees.

oxy system only occurred under a significant positive pressure potential at the inflow boundary (~50 mm). Even then, only the lower 5% of the fracture was wetted (Figure 5c).

5. Summary

A method for casting transparent glass replicas of rock fractures was developed. The glass casts obtained using this method provided close reproduction of major features of natural fracture topography. Some loss of fine-scale surface roughness (<5 μm) replication was revealed in laser profilometry and AFM results and is attributed to the particle size of the investment powder. The glass casts are generally more water wettable than epoxy casts and can also be treated to exhibit specific desired wettabilities. Thus, for visualization studies of multiphase fluid environments in fractures, glass casts are suitable to use for a wide range of natural fracture surface wettabilities. They can be used to study mechanisms controlling multiphase fluid flow and contaminant transport (including solutes, colloids, microorganisms, and nonaqueous phase liquids), to examine remediation techniques at small scale, and to conduct laboratory studies for enhancing petroleum recovery.

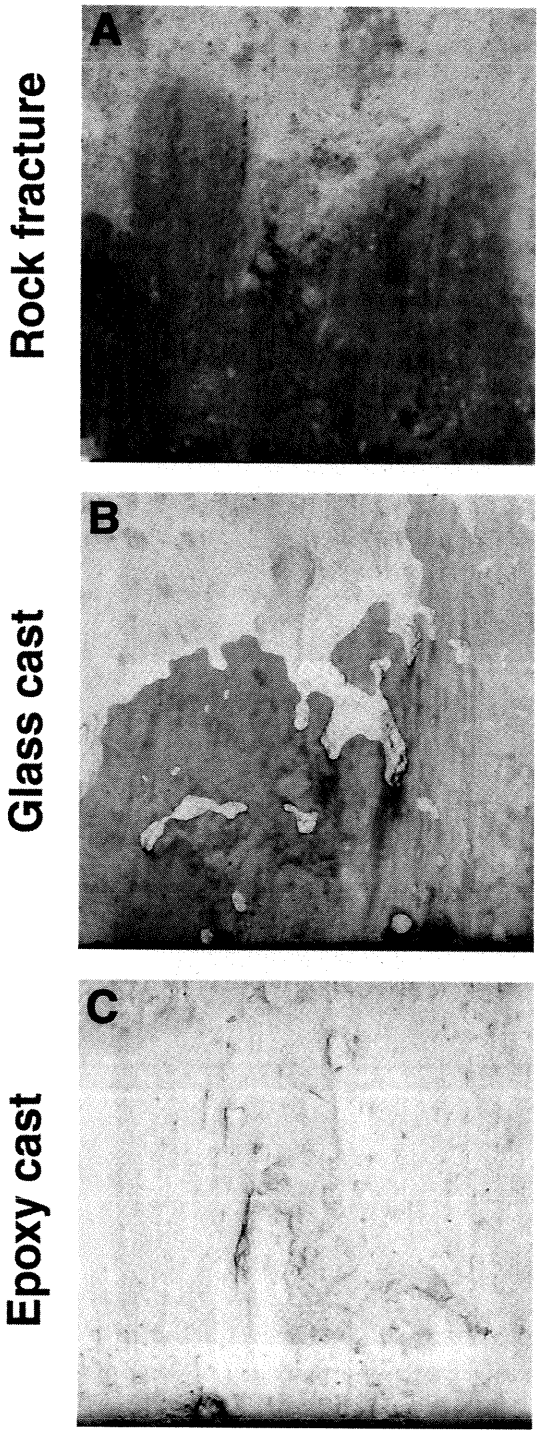

Figure 5. Imbibition of blue dyed water into fractures from the bottom edge. These examples are all 70 mm by 70 mm. (a) Wetting pattern on the gabbro, (b) glass cast, and (c) epoxy cast. Photographs were taken after 60 min of wetting. The rock and glass cast were wet with zero pressure potential at the inlet boundary, while +0.50 kPa pressure potential was required to initiate slight wetting of the epoxy cast.

Acknowledgments. This work was supported by the U.S. Department of Energy, Office of Basic Energy Sciences, Geosciences Research Program, under U.S. Department of Energy contract DE-AC03-76SF-00098. The authors thank Peter Persoff (LBNL) for providing the Dixie Valley rock fractures and epoxy casts. The authors are very appreciative for the helpful review comments by Michael J. Nicholl.

References

Bethel, F. T., and J. C. Calhoun, Capillary desaturation in unconsolidated beads, *Trans. Am. Inst. Min. Metall. Pet. Eng.*, *198*, 197–202, 1953.

Brown, S. R., Simple mathematical model of a rough fracture, *J. Geophys. Res.*, *100*(B4), 5941–5952, 1995.

Brown, S., A. Caprihan, and R. Hardy, Experimental observation of fluid flow channels in a single fracture, *J. Geophys. Res.*, *103*(B3), 5125–5132, 1998.

Cox, B. L., S. Finsterle, and J. S. Y. Wang, Experimental and numerical aqueous flow through a partially saturated fracture, in *Proceedings of the Sixth Annual International Conference on High-Level Radioactive Waste Management*, vol. 5, pp. 20–22, Am. Nucl. Soc., LaGrange Park, Ill., 1995.

Fourar, M., S. Bories, R. Lenormand, and P. Persoff, Two-phase flow in smooth and rough fractures: Measurement and correlation by porous-medium and pore flow models, *Water Resour. Res.*, *29*, 3699–3708, 1993.

Gatenby, W. A., and S. S. Marsden, Some wettability characteristics of synthetic porous media, *Prod. Mon.*, *22*, 5–12, 1957.

Geller, J., and K. Pruess, On water infiltration in rough-walled fractures, in *Proceedings of the Sixth Annual International Conference on High-Level Radioactive Waste Management*, vol. 5, pp. 23–25, Am. Nucl. Soc., LaGrange Park, Ill., 1995.

Gentier, S., Morphologie et comportment hydromecanique d'une fracture naturelle dans un granite sous constrainte normale, Ph.D. thesis, Univ. d'Orleans, Orleans, France, 1986.

Gentier, S., D. Billaus, and L. van Vliet, Laboratory testing of the voids of a fracture, *Int. J. Rock Mech. Rock Eng.*, *22*, 149–157, 1989.

Haghighi, M., B. Xu, and Y. C. Yortsos, Visualization and simulation of immiscible displacement in fractured systems using micromodels, 1, Drainage, *J. Colloid Interface Sci.*, *166*, 168–179, 1994.

Hakami, E., and N. Barton, Aperture measurement and flow experiments using transparent replicas of rock joints, in *Proceedings of the International Symposium on Rock Joints*, edited by N. Barton and O. Stephansson, pp. 383–390, A. A. Balkema, Brookfield, Vt., 1990.

Jennings, H. Y., Surface properties of natural and synthetic porous media, *Prod. Mon.*, *21*, 20–24, 1957.

Nicholl, M. J., and R. J. Glass, Wetting phase permeability in a partially saturated horizontal fracture, in *Proceedings of the Fifth Annual International Conference on High-Level Radioactive Waste Management*, vol. 4, pp. 2007–2019, Am. Nucl. Soc., LaGrange Park, Ill., 1994.

Nicholl, M. J., R. J. Glass, and S. W. Wheatcraft, Gravity-driven infiltration instability in initially dry nonhorizontal fractures, *Water Resour. Res.*, *30*, 2533–2546, 1994.

Persoff, P., and K. Pruess, Flow visualization and relative permeability measurements in transparent replicas of rough-walled rock fractures, in *High Level Radioactive Waste Management: Proceedings of the 4th International Conference*, vol. 2, pp. 2033–2041, Am. Soc. Civ. Eng., New York, 1993.

Persoff, P., and K. Pruess, Two-phase flow visualization and relative permeability measurement in natural rough-walled rock fractures, *Water Resour. Res.*, *31*, 1175–1186, 1995.

Power, W. L., and T. E. Tullis, The relationship between slickenside surfaces in fine-grained quartz and the seismic cycle, *J. Struct. Geol.*, *11*, 879–893, 1989.

Power, W. L., and T. E. Tullis, Euclidean and fractal models for the description of rock surface roughness, *J. Geophys. Res.*, *96*(B1), 415–424, 1991.

Reimus, P. W., B. A. Robinson, and R. J. Glass, Aperture characteristics, saturated fluid-flow, and tracer transport calculations for a natural fracture, in *Proceedings of the Fourth Annual International Conference on High-Level Radioactive Waste Management*, vol. 2, pp. 2009–2016, Am. Nucl. Soc., LaGrange Park, Ill., 1993.

Wan, J., T. K. Tokunaga, C. F. Tsang, and G. S. Bodvarsson, Improved glass micromodel methods for studies of flow and transport in fractured porous media, *Water Resour. Res.*, *32*, 1955–1964, 1996.

R. W. Connors, J. O'Neill, T. R. Orr, T. K. Tokunaga, and J. Wan, Earth Science Division, E. O. Lawrence Berkeley National Laboratory, 1 Cyclotron Road, MS 90-1116, Berkeley, CA 94720. (jwan@lbl.gov)

(Received November 30, 1998; revised September 17, 1999; accepted September 21, 1999.)